Molecular excitons in poly(*p*-phenylene-vinylene): a comparative study of PPV and an acetoxy substituted copolymer derivative

S. Forero Lenger [a,*], J. Gmeiner [a,b], W. Brütting [a,1]

[a] *Lehrstuhl Experimentalphysik II, Universität Bayreuth, Universitätsstr. 30, 95440 Bayreuth, Germany*
[b] *Bayreuther Institut für, Makromolekülforschung (BIMF), Universität Bayreuth, 95440 Bayreuth, Germany*

Abstract

With the aid of in-situ absorption spectroscopy we performed a comparative study of the precursor route poly(*p*-phenylene-vinylene) homopolymer and an acetoxy substituted copolymer derivative as a function of conversion temperature. It is shown that assuming a *trans-cisoid* conformation both polymers can be treated as arrays of *trans*-stilbene-like chromophores rendering a consistent description in the framework of molecular excitons. During conversion the intrachain geometry is retained and the energies of vibronic transitions are unchanged, while the respective intensities depend on the interchain distance. We find that the acetoxy substituent of the copolymer acts as interchain spacer supressing aggregation.

1. Introduction

During the last decade conjugated polymers have been studied extensively for their use in optoelectronic and photovoltaic applications [1]. One prominent representative of this material class is the precursor route poly(*p*-phenylene-vinylene) homopolymer (h-PPV). As the intra- and intermolecular structure inherited from its parent precursor is still unknown the photophysical properties of h-PPV are not deciphered completely yet. Traditionally the optical properties of h-PPV are interpreted in the framework of a distribution of intrachain segments of length l_s owing different effective electron delocalization lengths l_d [3]. In contrast to this, Hernández et al. [4] postulate a π-electron-pinning inside the aromatic parts of h-PPV and related oligomers, reducing the effective delocalization length along the polymer chain

* Corresponding author. Fax: +49-921-55-2621.
E-mail address: stefan.forero@future-carbon.de (S.F. Lenger).
[1] Present address: Lehrstuhl Experimentalphysik IV, Institut für Physik, Universitätsstrasse 1 Nord, 86135 Augsburg, Germany.

to a π-electron confinement length $l_c < l_d$. An increase of l_s should result in a saturation behaviour, e.g., in relative intensities or energy shifts, for $l_s > l_d$, l_c. A first systematic investigation of the conversion process of h-PPV was performed by Herold et al. [2]. With the aid of in-situ infrared and UV–vis spectroscopy they proposed a chemical and structural pathway from the precursor to h-PPV. Here we present for the first time a comparative study of h-PPV and an acetoxy substituted copolymer derivative (ac-PPV) by means of in-situ ultraviolet–visible spectroscopy (UV–vis) as a function of the conversion temperature T_{conv}. By in-situ tracing of the optical spectra of h-PPV and ac-PPV we show that the energy of UV–vis transitions is independent of the degree of substitution and therefore, does apparently not depend on chainlength. Consequently we support the picture of the π-electron confinement proposed by Hernández et al. [4]. The spectroscopic results allow a treatment following the framework of the molecular exciton as reviewed by McClure [5,6]. We also consider the influence of electronic interstate mixing as treated by Tinoco [7] and Rhodes [8]. Crucial parameters are recognized to be the interchain distance and the inter- and intrachain geometry of the polymers under study.

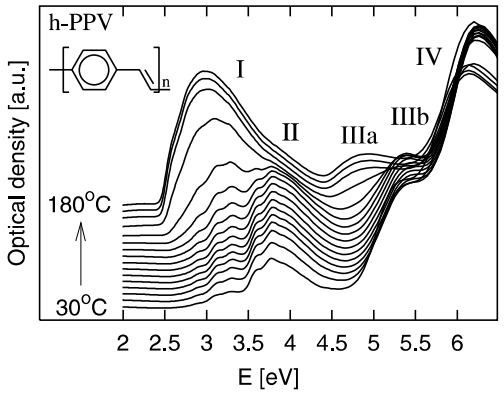

Fig. 1. In situ UV–vis spectra as a function of conversion temperature T_{conv} for h-PPV. A temperature increment of 10 °C was applied in time intervals of 1 h. For clarity the spectra are vertically shifted by a constant increment.

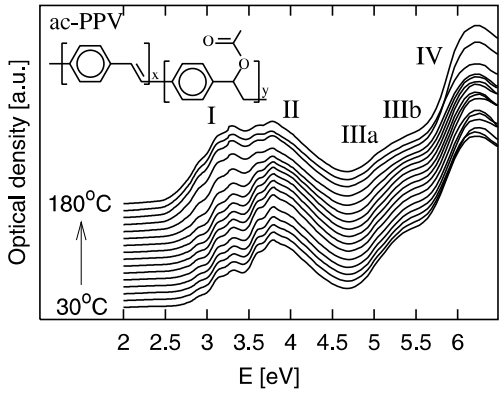

Fig. 2. In situ UV–vis spectra as a function of conversion temperature T_{conv} for ac-PPV. A temperature increment of 10 °C was applied in time intervals of 1 h. $y/(x+y) \approx 15$–20%. For clarity the spectra are vertically shifted by a constant increment.

2. Experimental

Two poly(*p*-phenylene-vinylene) polymers prepared via the chlorine-based sulfonium salt precursor route were characterized: the homopolymer (h-PPV) and a 15–20% acetoxy substituted copolymer derivative (ac-PPV) (see insets in Figs. 1 and 2). The molecular weight of both materials is about 10^5–10^6 g/mol ($\Rightarrow n \approx 10^3$–$10^4$ phenylene-vinylene units per chain) [10]. Concerning the synthesis of the homopolymer and its precursor we refer to [9] and [10]. The ac-PPV prepolymer was synthesized similar to the h-PPV precursor [10] but with an excess of the base lithium hydroxide. The polymer films (60–70 nm thick) were fabricated by a doctor blade technique [10] on quartz glass and then mounted in a heating cell with quartz windows under vacuum (0.01 mbar). At room temperature the heating cell was evacuated for an hour before the heating programme was started. Then the temperature was increased to 180 °C stepwise by 10 °C in time intervals of one hour. Spectra were taken in situ at the end of every heating step with a Perkin–Elmer Lambda2 UV–vis spectrometer. From in-situ infrared spectroscopy (IR) of CH_2 groups performed in the same manner (not shown here) we found that the substitution of the precursors with tetrahydrothiophenium and Cl decreases after evacuation from 100% to ca. 35% and after heating to 100 °C to less than 10%, in

good agreement with photoelectron spectroscopy results by Nguyen et al. [11].

3. Results and discussion

In Figs. 1 and 2 the in situ UV–vis spectra of h-PPV and ac-PPV are shown as a function of T_{conv}. The most important features are observed in both polymers and are denoted by roman numbers I–IV. Strikingly both polymers show identical vibronic progressions without any significant bathochromic shift (decrease in energy). Rather correlated hyper- and hypochromic shifts (increase and decrease of intensity, respectively) are observed: in the UV–vis spectra a presumable intensity transfer from the (IIIb) and (IV) bands to the (IIIa) and (I) bands takes place. We observe that in the range 50 °C $\leqslant T_{conv} \leqslant$ 100 °C the intensities of the absorption bands converge to a constant value, whereas further increase of T_{conv} causes considerable changes in intensities, for h-PPV up to 180 °C and for ac-PPV up to 140 °C. If one ignores the constant vibronic energies throughout the conversion process, in the model of distributed delocalization lengths [3] this behaviour is expected, because ac-PPV due to the acetoxy substitution should retain short conjugated segments. For h-PPV the distribution of the delocalization lengths should vary dynamically with advancing conversion from lower to higher l_d values. However, the above mentioned experimental results from IR spectroscopy rather suggest that the electron delocalization length l_d is comparable at the beginning and the end of the conversion in both polymers and therefore, shorter than the average intrachain segment length l_s imposed in ac-PPV by the acetoxy substitution. Thus l_d/l_s saturates at the very early stages of conversion and l_d can be replaced by l_c. This might explain why the vibronic transition energies in both polymers do not shift with increasing T_{conv}. As mentioned in the experimental section the main chemical processes take place for $T_{conv} \leqslant 100$ °C. In many cases UV–vis spectra of biopolymers, e.g., polynucleotides, show intensity redistributions upon reorganization of the nonconjugated chromophores on the polymer chains [7,8]. Consequently, we attribute the changes in the electronic characteristics of h-PPV and ac-PPV for $T_{conv} \geqslant 100$ °C to the aggregation behaviour of the polymerchains. Indeed, in this temperature region the conversion is predominantly viewed as an annealing process, which is obviously different in both polymers.

The observations made can be rationalized in the theoretical framework of the molecular exciton introduced by Davydov [12]. Obrzut et al. [13] first interpreted h-PPV on the basis of this excitonic model. However, only different states of substitution were treated and the hyper- and hypochromic shifts could not be explained in a satisfying manner. Herold et al. [2] proposed that due to the mainly syndiotactic structure of the prepolymer (neighbouring substituents are on opposite sides of the polymer chain), the h-PPV chain should isomerize from a *trans-cisoid* structure to the *trans-transoid* final conformation. In the former case the intrachain repeat unit is doubled in size as compared to the latter case (see Fig. 3). We argue that the *trans-cisoid* chain is the main final intrachain conformation for both h- and ac-PPV. Then the intrachain unitcell would roughly represent a two-stilbene-dimer with both monomers aligned in zig-zag geometry (*trans*-stilbene = TSB). At first we will sketch the theoretical model for an arbitrary pair of identical, nonconjugated and translationally inequivalent chromophores A and B following McClure [5] and Kasha et al. [15]. Thereafter the model will be applied to h-PPV and ac-PPV.

Let q_A and Q_A denote the electronic and nuclear coordinates for A. The Hamiltonian for this chromophore is written as $H_A = H_i(q_A, Q_A) + H_j(Q_A)$, where i stands for the electronic and j for the nuclear contributions. Further we define for A the vibronic wavefunctions $\psi_A = \psi(q_A, Q_A)\chi(Q_A)$ composed itself of electronic (ψ) and vibrational (χ) functions. An analogous treatment can be done for B. The ground state of the dimer AB is given by the wavefunction $\phi^0 = \psi_A^0\psi_B^0$. Excited states of the dimer exist in which the excitation m, n is either on A or B, namely $\phi^{m0} = \psi_A^m\psi_B^0$ or $\phi^{0n} = \psi_A^0\psi_B^n$. When both A and B are excited simultaneously we have the dimeric wavefunctions $\phi^{mn} = \psi_A^m\psi_B^n$. The Hamiltonian for the dimer is composed of the Hamiltonians of each chromophore and a chromophore–chromophore interaction potential:

$$H = H_A + H_B + V_{AB}. \quad (1)$$

The energy of the dimer ground state results from

$$E^0_{AB} = \int\int \phi^{0*}(H)\phi^0 \,\mathrm{d}q\,\mathrm{d}Q = E^0_A + E^0_B + D^0, \quad (2)$$

where E^0_A and E^0_B being the ground state energies of the single chromophores and D^0 the van der Waals energy lowering for the dimer ground state. Focusing on the excited dimeric states with one monomer excited to its state m the wavefunctions are described by $\phi^{m\pm} = \phi^{m0} \pm \phi^{0m}$. Two energy values for the excited state of the dimer AB are obtained:

$$E^{m\pm}_{AB} = \int\int \phi^{0*}(H)\phi^{m\pm}\,\mathrm{d}q\,\mathrm{d}Q = E^m + E^0 + D^m + \varepsilon^{m\pm}_{AB}, \quad (3)$$

where $E^0 = E^0_A = E^0_B$, $E^m = E^m_A = E^m_B$ and D^m is the van der Waals energy lowering for the dimeric excited state. The exciton splitting energy $\varepsilon^{m\pm}_{AB}$ constitutes the Coulomb interaction between the monomeric transition dipoles $\vec{\mu}^m_A(q_A, Q_A)$ and $\vec{\mu}^m_B(q_B, Q_B)$ that are separated by the distance vector $\vec{r}^m_{AB}$:

$$\varepsilon^{m\pm}_{AB} = \frac{(\mu^m)^2}{(r^m_{AB})^3} G^{m\pm}_{AB}, \qquad G^{m\pm}_{AB} \equiv (\cos\alpha - 3\cos\beta_A \cos\beta_B), \quad (4)$$

where μ^m stands for either $|\vec{\mu}^m_A|$ or $|\vec{\mu}^m_B|$. Therein we have the alignment angles $\alpha = \angle(\vec{\mu}^m_A, \vec{\mu}^m_B)$, $\beta_A = \angle(\vec{\mu}^m_A, \vec{r}^m_{AB})$, $\beta_B = \angle(\vec{\mu}^m_B, \vec{r}^m_{AB})$ being coplanar. The energetic difference between the ground and the excited state is:

$$E^{m\pm} = \Delta E^m + \Delta D^m + \varepsilon^{m\pm}_{AB}, \quad (5)$$

where $\Delta E^m = (E^m_A - E^0_A) = (E^m_B - E^0_B)$ and $\Delta D^m = (D^m - D^0)$. The total transition dipole moment $\vec{\mu}^m_{AB}$ of the dimer is obtained from the transition dipoles $\vec{\mu}^m_A$ and $\vec{\mu}^m_B$ by:

$$\vec{\mu}^{m\pm}_{AB} = \vec{\mu}^m_A \pm \vec{\mu}^m_B. \quad (6)$$

McRae and Kasha et al. [14,15] reviewed how the alignment of the transition dipole moments $\vec{\mu}^m_A$ and $\vec{\mu}^m_B$ influence the exciton splitting energy $\varepsilon^{m\pm}_{AB}$ and the oscillator strengths $f^{m\pm} \sim |\vec{\mu}^{m\pm}_{AB}|^2$. Here we are interested in a zig-zag configuration of the transition dipole moments. This results in both transitions $E^{m\pm}_{AB}$ to be allowed. From Eqs. 4 and 6 we find $f^{m\pm} \sim (1 \pm \cos^2\beta \mp \sin^2\beta)$ and $G^{m\pm}_{AB} = (\mp 1 \mp \cos^2\beta)$, where $\beta = |\beta_A| = |\beta_B|$. The total exciton splitting energy is

$$\Delta\varepsilon_{AB} = \frac{2(\mu^m)^2}{(r^m_{AB})^3} G^{m-}_{AB}. \quad (7)$$

We now return to h-PPV and ac-PPV. In Fig. 3 the proposed intra- and interchain geometry is shown. For simplicity we do not consider interchain translational shifts along the x-axis. Taking care to be sufficiently far from precursor- and aggregation-properties we apply the exciton description to our polymers for $T_{\mathrm{conv}} \geqslant 100$ °C, where both polymers have similar UV–vis characteristics and we suppose that $l_s > l_c$. Thus the spectrum for the isolated polymerchain is taken to be that at $T_{\mathrm{conv}} = 100$ °C. We then identify the lowest absorption bands (I) and (II) as arising from excitations spreaded over two phenylene rings resulting in transition moments $\vec{\mu}_u$ and $\vec{\mu}_v$ directing along the doublebond of the vinylene units and being perturbed by its stretching vibration as it is the case in TSB [6,16]. The Coulomb interaction between two such transition dipoles in the intrachain unit cell centered on the vinylene units and aligned in a zig-zag configuration is responsible for the splitting of (I) and (II). This exciton coupling mechanism is not expected for the other transitions. The absorption bands (IIIa), (IIIb) and (IV) are attributed to localized excitations of the phenylene rings in the dimers,

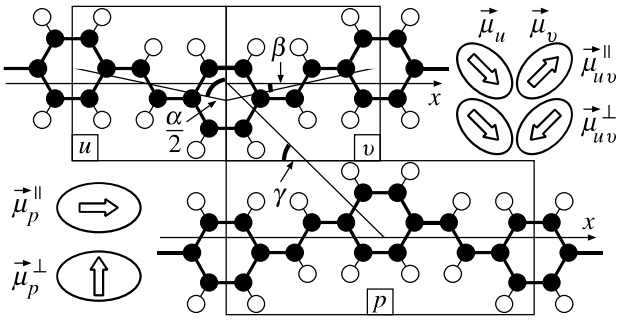

Fig. 3. Proposed intra- and intermolecular structure of *trans-cisoid* h-PPV. Two intrachain excitation sites u, v are shown arranged in zig-zag configuration along the chain axis x that lead to transitions $(\mathrm{I})^{\parallel}$, $(\mathrm{II})^{\perp}$; p denotes localized aromatic transitions $(\mathrm{IIIa,b})^{\perp}$, $(\mathrm{IV})^{\parallel}$ in the dimers.

associated with transition moments $\vec{\mu}_p$. The polarizations are chosen as predicted in [17–19]: (I), $\vec{\mu}_{uv}^{\parallel} = (\vec{\mu}_u + \vec{\mu}_v)$; (II), $\vec{\mu}_{uv}^{\perp} = (\vec{\mu}_u - \vec{\mu}_v)$; (IIIa,b), $\vec{\mu}_p^{\perp}$ and (IV), $\vec{\mu}_p^{\parallel}$.

In order to apply the exciton model to h- and ac-PPV we fitted the UV–vis spectra with Gaussian functions for different T_{conv} (see Fig. 4). The transition energies for (IIIa,b) and (IV) are $E^{(IIIa)} = 4.9$ eV, $E^{(IIIb)} = 5.3$ eV and $E^{(IV)} = 6.2$ eV, respectively. Absorption bands (I) and (II) were each resolved by a separate set of Gaussian functions modeling the vibronic structure. The vibronic spacing for (I) is about 1400 cm^{-1} and for (II) about 1600 cm^{-1}. From the lowest energy of each Gaussian set we find $E^{(I)} = 2.6$ eV and $E^{(II)} = 3.2$ eV. This results in an exciton coupling term of about $\Delta\varepsilon_{uv} = 0.6$ eV. The occurrence of vibronic progressions for (I) and (II) hints to slight changes in bond force constants and nuclear equilibrium positions. As the vibronic spacing is smaller than the exciton coupling energy and independent of intensity the coupling can be viewed in good approximation to be moderately strong [20]. From the intensity ratio $f^{(I)}/f^{(II)} = \tan^2\beta$ (which means f^{m-}/f^{m+}) we calculate $\beta = 24°$. Via Eq. 7 we check the distance between the chromophores to be $|\vec{r}_{uv}| = 6.5$ Å by setting $|\vec{\mu}^m| = |\vec{\mu}_{TSB}| = 6.7$ D. The latter value is taken from [21] and the distance $|\vec{r}_{uv}|$ is in excellent agreement with the X-ray data presented in [22]. In Fig. 4 we also show that by keeping the vibronic energies constant only an increase of oscillator strength must be considered to model the UV–vis spectra. Therefore, the intramolecular geometry of the polymer chains shown in Fig. 3 must be recognized as an energetically stable configuration throughout the conversion process.

In Fig. 5 we compare the integrated intensities (in particular the integrated Gaussian functions) of the different absorption bands as a function of T_{conv}. Considerable hypo- and hyperchromic shifts appear for $T_{conv} > 100$ °C. We account for them by allowing a mixing of the ground state wavefunction ϕ^0 with doubly excited dimeric states ϕ^{mn} and dimeric excited states ϕ^m with other singly excited states ϕ^n:

$$\varphi^0 = \phi^0 + \sum_{mn} a_{mn}\phi^{mn}, \tag{8}$$

$$\varphi^\dagger = \phi^m + \sum_{n} b_n\phi^n. \tag{9}$$

As we are now interested in interchain dimer–dimer interactions we have to consider the interchain geometry. Polymer chain stacking in herringbone fashion renders one chain with six neighbours at equal distances. So, a dimer in the central chain will have $N_k = 12$ dimeric neighbours, namely two on each other chain. If we take the dimers to be ≈ 13 Å long and a typical crystallite to size ≈ 300 Å in length [23] then the

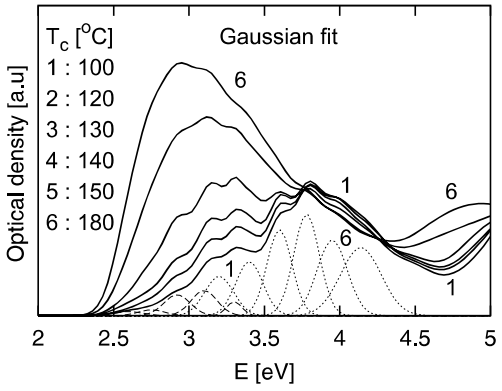

Fig. 4. Calculated UV–vis spectra for different T_{conv} in the range of bands (I), (II). Curves 1–4 constitute the conversion of ac-PPV and curves 1–6 the conversion of h-PPV. By going from 1 to 6 the vibronic energies were kept fixed and only oscillator strengths were increased.

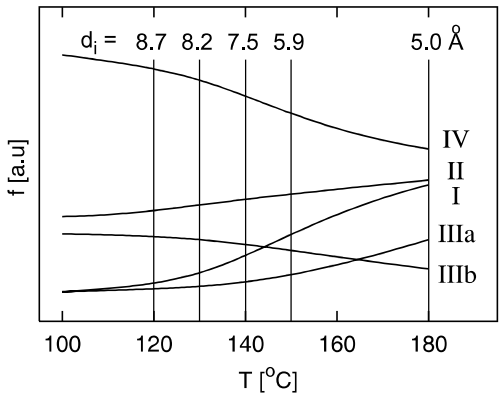

Fig. 5. Integrated intensities for UV–vis absorption bands (I), (II), (IIIa), (IIIb) and (IV) as a function of the conversion temperature T_{conv}. The vertical lines indicate the predicted respective interchain distances $d_i(T_{conv})$.

chainlength in the aggregate will be equivalent to $N_l \approx 23$ dimers in line. According to Tinoco [7] and Rhodes [8] the evaluation of $E^{\dagger} = \int \varphi^0(H)\varphi^{\dagger}$ renders to first order and in dipole–dipole approximation the total intensity f_t^m for the transition m:

$$f_t^m = f_l^m N_l - B\frac{f_l^m N_l f_k^n N_k}{(E^n)^2 - (E^m)^2}\frac{G_{lk}^{mn}}{(r_{lk}^{mn})^3}, \qquad G_{lk}^{mn} \equiv (1 - 3\cos^2\gamma_{lk}^{mn}), \tag{10}$$

where $B = 6.6 \cdot 10^2$ ÅeV and E^m, E^n are the energies of transitions m, n, respectively. The term G_{lk}^{mn} constitutes dipole–dipole interaction of parallel aligned transition dipoles [15]. Consequently the transition intensity f_l^m of a free dimer l to state m will be reduced or increased to the total intensity f_t^m by the polarization dipole $\sim f_k^n$ of neighbouring dimers k in dependence on the relative orientation ($\gamma_{lk}^{mn} = \angle(\vec{\mu}_{l,k}^{m,n}, \vec{r}_{lk}^{mn})$) of both transition dipoles $\vec{\mu}_l^m$ and $\vec{\mu}_k^n$. If we denote by d_i the interchain distance we can write the interdimer distance as $\vec{r}_{lk}^{mn} = d_i/\sin\gamma_{lk}^{mn}$ and it follows from Eq. 10 that:

$$f_t^m - f_l^m = -B\frac{f_l^m f_k^n}{(E^n)^2 - (E^m)^2}\frac{g_{lk}^{mn}}{d_i^3}, \qquad g_{lk}^{mn} \equiv N_l N_k G_{lk}^{mn}\sin^3\gamma_{lk}^{mn}. \tag{11}$$

Considering $\tan\gamma_{lk}^{mn} = d_i/(6.5\ \text{Å})$ the expression allows the determination of d_i from the experimental f- and E-values. For a hyperchromic shift it is required that $g_{lk}^{mn} < 0$. This restricts γ_{lk}^{mn} to be in the range 0°–54.7° and d_i to be <9 Å. Any further lowering of the interchain distance will result in a hyperchromic shift. For h-PPV we consider the first of two cases of intensity transfer: 1. (I)↔(IV); 2. (IIIa)↔(IIIb). The dimeric transition dipoles $\vec{\mu}_{uv}^{\parallel} = \vec{\mu}_{uv}^{(\mathrm{I})}$ and $\vec{\mu}_p^{\parallel} = \vec{\mu}_p^{(\mathrm{IV})}$ are centered on the phenylene rings. As reference spectrum for the isolated polymerchain we again take that at $T_{\mathrm{conv}} = 100$ °C, which renders $f_l^m \equiv f_{uv}^{(\mathrm{I})}$. By increasing the temperature T_{conv} the values $f_t^m \equiv f_t^{(\mathrm{I})}(T_{\mathrm{conv}})$ and $f_k^n \equiv f_p^{(\mathrm{IV})}(T_{\mathrm{conv}})$ will change as $d_i(T_{\mathrm{conv}})$ is decreased. Then, from Eq. 11 we can readily obtain the interchain distance for different T_{conv}. The calculated $d_i(T_{\mathrm{conv}})$-values are inserted into Fig. 5. From these results we conclude that the average interchain distance in ac-PPV must be ≈ 8.0 Å, while in h-PPV the polymer chains approach each other to 5.0 Å at the final stage of conversion. The latter value is also in very good agreement with X-ray diffraction experiments on stretched [22] and unstretched [24] h-PPV.

4. Conclusions

We have shown that the effective conjugation length is equal in h-PPV and ac-PPV but shorter than that imposed by the acetoxy substitution in ac-PPV. In particular the assumption that it is not longer than a *trans*-stilbene unit seems reasonable if electrostatic interaction between two such units is significant. A *trans-cisoid* structure for h-PPV and ac-PPV provides a consistent picture for a molecular exciton on an intrachain zig-zag-dimer. The energies of UV–vis transitions are fixed by the intrachain geometry and the transition probabilities are influenced by dimeric interchain interaction in both materials. The great difference between both polymers is that due to the acetoxy substitution in ac-PPV the degree of interchain aggregation is considerably lower as in the case of h-PPV. Indeed the acetoxy group must be viewed as an interchain-spacer and not as a unit breaking the intrachain conjugation.

Acknowledgements

We thank D. Scherer for stimulating discussion. This work was supported by DFG Sonderforschungsbereich 481.

References

[1] T.A. Skotheim, R.L. Elsenbaumer, J.R. Reynolds (Eds.), Handbook of Conducting Polymers, Marcel-Dekker, New York, 1998.
[2] M. Herold, J. Gmeiner, M. Schwoerer, Polym. Adv. Technol. 10 (1999) 251.
[3] E. Mulazzi, A. Ripamonti, J. Wery, B. Dulieu, S. Lefrant, Phys. Rev. B 60 (1999) 16519.
[4] V. Hernández, C. Castiglioni, M. Del Zoppo, G. Zerbi, Phys. Rev. B 50 (1994) 9815.
[5] D.S. McClure, Can. J. Chem. 36 (1958) 59.

[6] D.S. McClure, Sol. State. Phys. 8 (1959) 1.
[7] I. Tinoco, J. Am. Chem. Soc. 82 (1960) 4785.
[8] W. Rhodes, J. Am. Chem. Soc. 83 (1961) 3609.
[9] R.A. Wessling, J. Pol. Sci. Symp. 72 (1985) 55.
[10] M. Herold, J. Gmeiner, M. Schwoerer, Acta Polym. 45 (1994) 392.
[11] T.P. Nguyen, P. Le Rendu, V.H. Tran, P. Molinié, Polym. Adv. Technol. 9 (1998) 101.
[12] A.S. Davydov, Theory of Molecular Excitons, Plenum Press, New York, 1971.
[13] J. Obrzut, F.E. Karasz, J. Chem. Phys. 87 (1987) 2349, see also 6178.
[14] E.G. McRae, M. Kasha, Physical Processes in Radiation Biology, Academic Press, New York, 1964, p. 23.
[15] M. Kasha, H.R. Rawls, M. Ashraf El-Bayoumi, Pure Appl. Chem. 11 (1965) 371.
[16] R.H. Dyck, D.S. McClure, J. Chem. Phys. 36 (1962) 2326.
[17] M.J. Rice, Y.N. Gartstein, Phys. Rev. Lett. 73 (1994) 2504.
[18] Y.N. Gartstein, M.J. Rice, E.M. Conwell, Phys. Rev. B 52 (1995) 1683.
[19] M. Chandross, S. Mazumdar, S. Jeglinski, X. Wei, Z.V. Vardeny, E.W. Kwock, T.M. Miller, Phys. Rev. B 50 (1994) 14702.
[20] W.T. Simpson, D.L. Peterson, J. Chem. Phys. 26 (1957) 588.
[21] Z.G. Soos, S. Ramasesha, D.S. Galvão, S. Etemad, Phys. Rev. B 47 (1993) 1742.
[22] D. Chen, M.J. Winokur, M.A. Masse, F.E. Karasz, Phys. Rev. B 41 (1990) 6759.
[23] D.D.C. Bradley, J. Phys. D 20 (1987) 1389.
[24] H.V. Shah, J.I. Scheinbeim, G.A. Arbuckle, Macromolecule 32 (1999) 605.